Liquid Crystals
Publication details, including instructions for authors and subscription information:
http://www.informaworld.com/smpp/title~content=t713926090

The electrooptics of smectic C liquid crystals

M. P. Petrov[a]; A. G. Petrov[a]; G. Pelzl[ab]
[a] Institute of Solid State Physics, Sofia, Bulgaria [b] Sektion Chemie der Martin-Luther-Universität, Germany

To cite this Article Petrov, M. P. , Petrov, A. G. and Pelzl, G.(1992) 'The electrooptics of smectic C liquid crystals', Liquid Crystals, 11: 6, 865 — 886
To link to this Article: DOI: 10.1080/02678299208030691
URL: http://dx.doi.org/10.1080/02678299208030691

LIQUID CRYSTALS, 1992, VOL. 11, NO. 6, 865–886

The electrooptics of smectic C liquid crystals

by M. P. PETROV*, A. G. PETROV and G. PELZL†
Institute of Solid State Physics, Bull. Lenin 72 1784 Sofia, Bulgaria
† Sektion Chemie der Martin-Luther-Universität,
4020 Halle/5, Mühlpforte 1, Germany

(*Received 24 April 1991; accepted 25 October 1991*)

A theoretical description of the electrodynamical instability for the initial and the fundamental domain regimes in smectic C liquid crystals is presented. On the basis of the bi-axial aspects of the problem, a dependence of the threshold field, charge and curvature relaxation times on the director **n** tilt angle (ω) were found. It is demonstrated that the electrodynamical instability is a priority of the C_1 type smectics, where the director tilt angle is temperature independent in the smectic C temperature range. It was found that the dielectric reorientation processes are stimulated mainly in C_2 smectics, where the director tilt angle is small and temperature dependent. The role of the sign and the magnitude of the dielectric anisotropy on the character of the electrooptic responses (pure electrohydrodynamic instability, pure dielectric reorientation or a mixture of the two) is discussed.

1. Introduction

The electrooptic behaviour of smectic C liquid crystals in AC and DC electric fields has been studied mainly in two directions: (i) the pure dielectric reorientation (or Fredericksz transition [1, 2] and the electrohydrodynamical instability [3–6]. There are very specific characteristics of a smectic C phase due to the more complex structure of this phase. A typical peculiarity of the S_C is the restriction of the director **n** to rotate (or reorient) around a cone with apex 2ω inside the layers; ω is the tilt angle between **n** and the layer normal **N**. The **n** rotation does not change the free energy of the system nor the interlayer distance. The layers are preserved in weak electric fields, since the charge flow is restricted (in the absence of texture defects) inside the smectic layers [7]. The layer destruction starts at very high DC and AC electric fields and some turbulent motions similar to the dynamic scattering in nematics has been observed [6]. The elastic properties of a smectic C [8, 9] phase is another specificity important for the electrooptics. At some specific boundary conditions the number of relevant Saupe elastic constants could be reduced to just two. Up to now, there is no useful hydrodynamic theory since the viscosity coefficients describing smectic C phases are numerous [10]. An effective important viscosity coefficient is the rotational viscosity ν connected with **n** rotation on the so-called easy cone.

The electrooptics of the smectic C depend mainly on the smectic C type; until now two types of smectic C phase [11] are known. The first type denoted as C_1 is characterized by a tilt angle ω which is temperature independent in the smectic C temperature range. An example of this type of smectic C_1 are the 4-*n*-alkyloxybenzoic acids with $n > 7$ and the 4,4′-di-*n*-alklyoxyazoxybenzenes. The electrohydrodynamic instability has been investigated in the smectic C_1 type. The second type of smectic C

* Author for correspondence.

(C_2) is characterized by a comparatively small tilt angle, which is temperature dependent in the S_C range. This type always forms below a smectic A phase. The instability in the smectic C_2 has not been investigated up to now, but the electrooptic effects related to the Fredericksz transition have been investigated mainly in this smectic type [1].

The S_C textures formed with identical boundary conditions (planar, homeotropic, tilted) are different for the C_1 and C_2 smectic types. For S_C, the most typical texture is composed of local single monocrystals with a planar orientation. The layers in such a texture are vertical in the absence and in the presence of an electric field, as demonstrated in [12]. In a planar oriented smectic C the infinite number of **n** positions on the cone reduces to two and we can observe only two directions of the vertical layers making an angle ω with the rubbing direction. The interpretation of the electrooptics in smectic C can be valuable only in the frame of a single local monocrystal. The texture in S_{C_2} with planar or tilted orientations is the broken variant of that for a smectic A. So the broken confocal texture is the most typical for planar or tilted smectic C_2.

Before the investigation [13–21] the textural, elastic and optical properties of the ferroelectric S_C^* as well as the achiral smectic C phases were only analysed assuming the existence of a flat layer structure. Recently in [13], by means of high resolution X-ray measurements, experimental evidence was reported for the existence of several types of a distorted local layer structure in the so-called surface stabilized ferroelectric liquid crystals. Rieker *et al.* [14] reported measurements for DOBAMBC and found a chevron as well as a uniformly tilted layer structure in the surface stabilized state. A chevron layer structure has also been suggested earlier by Pelzl *et al.* [1] for some substances of smectic C_2 type. According to Nakagawa's solution model [19], the chevrons result from the sliding of the molecules when the sample is cooled from S_A to S_C^* (or S_{C_2}). As was found [16] for a material which shows N* and S_C^* phases with a relatively large director tilt angle of 42°, the layer tilt angle is negligibly small and is much smaller than the director tilt angle. So, in materials of S_{C_2} type the chevrons or the uniform layer tilting are more favourable than for the S_{C_1} type, and specially for S_{C_1} possessing a relatively large director tilt angle. By X-ray experiments [12], neither chevrons nor uniform tilt layer distortion were observed in such materials. The experimental fact that the electrohydrodynamic instability was observed mainly in the substances with S_{C_1} phases strongly reflects the presence of vertical or flat planes of the layers at planar orientation of these materials.

A very important characteristic for the electrooptic behaviour of the smectic C phase is the biaxiality [22–24]. The value of the biaxiality increases with the tilt angle starting from zero at the $T_{S_CS_A}$ transition. So, in S_{C_2} type where the tilt angle is smaller than that of S_{C_1}, the biaxiality could be neglected, but in S_{C_1} type where ω is about 45° for some substances, the biaxiality is a decisive characteristic. The biaxiality of the smectic C phase and specially S_{C_1} leads to the different presentations of the important parameters in the electrooptics, namely the dielectric constant and the electroconductivity [25]. Having in mind these peculiarities of S_C which are not manifested by nematics and the other uniaxial smectics, we present the electrooptics of a smectic C phase at pure dielectric reorientation and at the electrohydrodynamic instability.

2. Theory

The theory of the magnetic field director reorientation (Fredericksz transition) of a smectic C phase was presented by Rapini [26] and later by Meirovich *et al.* [27] before

any experimental observations. The electric analogue of this transition has been studied experimentally and theoretically by Pelzl *et al.* [1, 2] in the smectic C_2 for some substances with positive dielectric anisotropy ($\Delta\varepsilon = \varepsilon_{\parallel} - \varepsilon_{\perp}$) where a uniaxial approximation is assumed and for a high frequency (2 kHz). The electrohydrodynamic instability expressed by domain lines has never been presented in the literature for smectic C_2.

The instability in S_{C_1} and two domain instability regimes were found: initial or low-frequency and fundamental or high frequency [5–7]. There is no theory for these instabilities so far. One of the reasons for the lack of a theory was that many details of these instabilities were not clear: for example, if the layers are undistorted during the instability, and the flow restriction inside the layers. Recent investigations [7] demonstrated the layer position and a periodic tilt coupled to a cellular flow restricted inside the smectic layer. They have also found that nematic-like bend-twist or bend elastic constants participate in the electrohydrodynamic instability. The permeation effect (the charge moving across the layers) has also been considered as a slow process compared to the period of the AC electric field.

Here we shall describe the instability for smectic C phases on the basis of present knowledge. As a first step, we shall consider the instability for S_C phases with a large tilt angle ω, where the biaxiality is more pronounced. As a second step, we shall adopt the considerations for S_C substances with different signs and magnitude of their dielectric anisotropies and we shall demonstrate that the threshold for pure dielectric reorientation (Fredericksz transition) and that of the instability are connected by some parametric constants of the substances.

2.1. *The low-frequency initial domain regime*

Since S_{C_1} is a locally biaxial system, the dielectric tensor in a local frame of reference has three different principal components ε_1, ε_2 and ε_3 with the principal axes, as follows (see figure 1): $\varepsilon_3 \rightarrow \mathbf{n}$, $\varepsilon_2 \rightarrow \mathbf{n} \times (\mathbf{N} \times \mathbf{C})$ (where $\mathbf{N}$ is the layer normal and $\mathbf{C}$ is the $\mathbf{n}$ projection on the layer plane) and $\varepsilon_1 \rightarrow \mathbf{N} \times \mathbf{C}$. In figure 1, θ is the polar angle and φ is the azimuthal angle expressing the $\mathbf{n}$ deviation from the rubbing or easy direction $\mathbf{R}$. τ is an axis on the xy plane coinciding with the $\mathbf{n}$ projection on this plane. Because of the anchoring forces, the initial director position (before electric excitation) points the rubbing direction. Using a laboratory cartesian frame (where oy is in the smectic layer planes (s) and ox coincides with the layer normal) after transforming to the local frame of reference (ζ, η, ξ) and assuming small θ and φ, we can simplify the presentation of $\boldsymbol{\varepsilon}$ in the first order. ϕ is the planar angle of the C rotation, and is connected with the angles ϕ and ω by the relation

$$\sin\phi = \sin\theta / \sin\omega.$$

From the geometry chosen by us in figure 1,

$$\omega' = \omega - \varphi = \omega(1 - \phi^2)$$

is the angle between the $\mathbf{n}$ projection and the x axis. Accordingly $\boldsymbol{\varepsilon}$ can be written in the xyz system as

$$\boldsymbol{\varepsilon} = \begin{pmatrix} \varepsilon_3\cos^2\omega + \varepsilon_2\sin 2\omega & (\varepsilon_2 - \varepsilon_3)\sin 2\omega/2 & (\varepsilon_3 - \varepsilon_1)\theta\cos\omega \\ (\varepsilon_2 - \varepsilon_3)\sin 2\omega/2 & \varepsilon_3\sin^2\omega + \varepsilon_2\cos^2\omega & -(\varepsilon_3 - \varepsilon_1)\theta\sin\omega \\ (\varepsilon_3 - \varepsilon_1)\theta\cos\omega & -(\varepsilon_3 - \varepsilon_1)\theta\sin\omega & \varepsilon_1 \end{pmatrix}. \tag{1}$$

to first order where $\Delta\varepsilon = \varepsilon_3 - \varepsilon_1$.

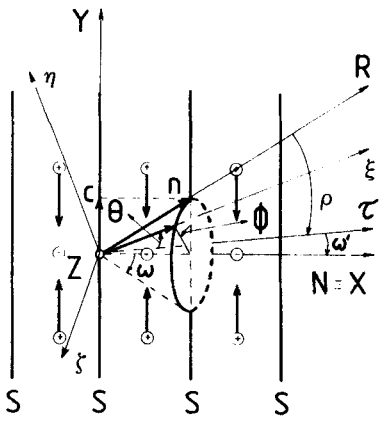

Figure 1. The smectic C director **n** presentation at the initial domain regime. **n** is connected with the laboratory and local $(0, \xi, \eta, \zeta)$ coordinate systems. The easy cone of the **n** reorientation is demonstrated. The layers (S) are vertical to the substrate planes. **N** is the layer normal and should be parallel to the substrate plane only for the cases where there are no chevron or uniformly tilted layer distortions. The **c** director is the **n** projection on the layer plane. ω is the tilt antle between **n** and the layer normal **N**. The x axis is perpendicular to the layer plane and coincides with **N**. The layer plane is the yz plane, **R** is the rubbing direction. θ and φ are the **n** polar angles. φ is the azimuthal angle of the **n** deviation from the rubbing direction **R**. τ is an axis in the xy plane. θ is the angle between τ and **n** at some position on the cone. ϕ presents the **c** rotation and is in the yz plane $\omega' = \omega - \varphi$ is presented in the text. The charge distribution inside the layers is also shown.

In the local frame the electric conductivity tensor also has three different principal components $(\sigma_1, \sigma_2, \sigma_3)$. The biaxiality of the system implies different local frames of the two tensors $\boldsymbol{\sigma}$ and $\boldsymbol{\varepsilon}$ [27] as well. The principal axes of $\boldsymbol{\sigma}$ for symmetry reasons are chosen to be: $\sigma_3 \rightarrow \mathbf{N}$, $\sigma_2 \rightarrow \mathbf{C}$ and $\sigma_1 \rightarrow \mathbf{N} \times \mathbf{C}$. We keep in mind that the electric conductivity is much less perpendicular to the smectic layers than inside the layers. We can accept then $\sigma_3 \approx 0$ and for small θ since

$$\sin\phi = \sin\theta / \sin\omega,$$

we obtain for $\boldsymbol{\sigma}$ in the xyz system:

$$\boldsymbol{\sigma} = \begin{pmatrix} 0 & 0 & 0 \\ 0 & \sigma_2 & (\sigma_2 - \sigma_1)\theta/\sin\omega \\ 0 & (\sigma_2 - \sigma_1)\theta/\sin\omega & \sigma_1 \end{pmatrix}, \tag{2}$$

where we assume $\Delta\sigma_b = \sigma_1 - \sigma_2$ as a first approximation to the anisotropy in the electroconductivity for the local biaxiality of the smectic C system.

We describe the electrohydrodynamic instability problem introducing time dependent equations, where the charge relaxation time and the orientational response time of the liquid crystal are taken into account. Applying the continuity equation for the electric current **J** (or the conservation equation for the charges) and for the electric induction **D**, we have [28]

$$\left.\begin{aligned} \dot{q} + \operatorname{div}\mathbf{J} = 0, \qquad & \mathbf{J} = \boldsymbol{\sigma}\mathbf{E}, \\ \operatorname{div}\mathbf{D} = q/\varepsilon_0, \qquad & \mathbf{D} = \boldsymbol{\varepsilon}\mathbf{E}. \end{aligned}\right\} \tag{3}$$

The electric field (in our case AC) is applied in the z direction parallel to the smectic layer plane. We assume that the eventual fluctuations induce a space charge q which in turn induces a flow restricted in the layers, and y component $E_y(y)$ of the total electric field. We shall omit the x component of the electric field; so $E(0, E_y, E_z)$. All of the possible director fluctuations are also restricted to a director $\mathbf{n}$ rotation on the easy cone as shown in figure 1, and bend–twist deformations are stimulated. Using the fundamental fluctuations propagating in the yz plane, i.e. $\theta(y)$ and $E_y(y)$

$$\left.\begin{aligned} \dot{q}+\partial J_y/\partial y=0, \\ \partial D_y/\partial y=q/\varepsilon_0. \end{aligned}\right\} \tag{4}$$

Taking $\boldsymbol{\varepsilon}$ and $\boldsymbol{\sigma}$ from equations (1) and (2), we find

$$J_y=\sigma_2 E_y+(\Delta\sigma_b/\sin\omega)\theta E_z,$$

$$D_y=\tfrac{1}{2}(\varepsilon_2-\varepsilon_3)\sin 2\omega E_x+(\varepsilon_3\sin^2\omega+\varepsilon_2\cos^2\omega)E_y-(\varepsilon_3-\varepsilon_1)\theta\sin\omega E_z.$$

Substituting $\psi=\partial\theta/\partial y$, the local director curvature, and $E_z\equiv E$, we obtain

$$\dot{q}+\sigma_2\partial E_y/\partial y+(\Delta\sigma_b/\sin\omega)\psi E=0,$$

$$\frac{q}{\varepsilon_0}=\tfrac{1}{2}(\varepsilon_2-\varepsilon_3)\sin 2\omega\frac{\partial E_x}{\partial y}+(\varepsilon_3\sin^2\omega+\varepsilon_2\cos^2\omega)\frac{\partial E_y}{\partial y}-(\varepsilon_3-\varepsilon_1)\sin\omega\psi E. \tag{5}$$

After calculating

$$\frac{\partial E_x}{\partial y}=\frac{\cos^2\omega(\varepsilon_2-\varepsilon_3)2(\varepsilon_3-\varepsilon_1)\sin^2\omega E\psi+[2(\varepsilon_2-\varepsilon_3)\sin^2\omega+(\varepsilon_1-\varepsilon_2)]\partial E_y/\partial y}{2(\varepsilon_2-\varepsilon_3)\cos^2\omega+(\varepsilon_1-\varepsilon_2)} \tag{6}$$

and

$$\partial E_y/\partial y=q(\varepsilon_0\tilde{\varepsilon}_\omega+\varepsilon_\omega\sin\omega E\psi), \tag{7}$$

we obtain

$$\dot{q}+\sigma_2 q/\tilde{\varepsilon}_\omega\varepsilon_0+\left(\frac{\sigma_1-\sigma_2}{\sin\omega}+\sigma_2\varepsilon_\omega\sin\omega\right)E\psi=0, \tag{8}$$

where

$$\tilde{\varepsilon}_\omega=\frac{2\varepsilon_1(\varepsilon_2-\varepsilon_3)\cos^2\omega+\varepsilon_3(\varepsilon_1-\varepsilon_2)}{2(\varepsilon_2-\varepsilon_3)\cos^2\omega+(\varepsilon_1-\varepsilon_2)}=\frac{\varepsilon_1\varepsilon_2-\varepsilon_3\varepsilon_2}{\varepsilon_1-\varepsilon_2}=\varepsilon_2;\quad \text{for}\quad \omega=\frac{\pi}{4} \tag{9}$$

and

$$\varepsilon_\omega=\frac{(\varepsilon_3-\varepsilon_1)(\varepsilon_1-\varepsilon_2)}{2(\varepsilon_2-\varepsilon_3)\cos^2\omega+(\varepsilon_1-\varepsilon_2)}=\varepsilon_2-\varepsilon_1;\quad \text{for}\quad \omega=\frac{\pi}{4}. \tag{10}$$

For comparison with the nematic electrohydrodynamic instability [28] we write the known charge balance equation:

$$\dot{q}+q/\tau+\sigma_H E\psi=0,$$

where

$$\tau^{-1}=4\pi\sigma_{\|}/\varepsilon_{\|}$$

is the dielectric relaxation time for charges and

$$\sigma_H = \sigma_{\parallel}\left(\frac{\varepsilon_\perp}{\varepsilon_{\parallel}} - \frac{\sigma_\perp}{\sigma_{\parallel}}\right).$$

The symbols $\parallel$ and $\perp$ mean the values of ε and σ along the director $\mathbf{n}$ and perpendicular to it in a uniaxial system such as a nematic. The charge balance equation in the nematics relates the charge q to the curvature of the director ψ. In equation (8) we have for a smectic C phase the same relation between q and ψ, and due to the biaxiality

$$\tau_C^{-1} = \sigma_2/\tilde{\varepsilon}_\omega \varepsilon_0, \tag{11}$$

where it is seen that the charge relaxation time in S_C depends on the tilt angle ω by $\tilde{\varepsilon}_\omega$. The second parameter from equation (8) corresponding to σ_H is

$$\sigma_C = (\sigma_1 - \sigma_2/\sin\omega + \sigma_2 \varepsilon_\omega \sin\omega), \tag{12}$$

where the tilt angle dependence is also shown.

The next step to describe the instability is the curvature director equation which follows from the equation of motion [28]

$$\rho dV/dt = -\mathrm{Div}(\rho \mathbf{VV}) + \mathrm{Div}(\boldsymbol{\sigma} + \boldsymbol{\sigma}') + qE, \tag{13}$$

where $\boldsymbol{\sigma}$ and $\boldsymbol{\sigma}'$ are the elastic and viscous stress tensors, respectively.

First, we consider the torque balance taking into account that the viscous torque (as the frictional one exerted upon the overall hydrodynamic motion by the director) should balance the sum of the elastic and dielectric torques. So, the equation for the torque balance is

$$\boldsymbol{\Gamma}^{el} + \boldsymbol{\Gamma}^{diel} + \boldsymbol{\Gamma}^{visc.} = 0. \tag{14}$$

The $\mathbf{n}$ components for small θ are $(\cos\omega, \sin\omega, \theta)$. The elastic torque ($\boldsymbol{\Gamma}^{el.}$) is

$$\boldsymbol{\Gamma}^{el.} = \mathbf{n} \times \mathbf{h}_{el.}, \tag{15}$$

where

$$\mathbf{h}_{el.} = K_{11}\,\mathrm{grad}\,\mathrm{div}\,\mathbf{n} - K_{22}[T\,\mathrm{rot}\,\mathbf{n} + \mathrm{rot}(T.\mathbf{n})] + K_{33}[(\mathrm{rot}\,\mathbf{n}) \times B + \mathrm{rot}(B \times \mathbf{n})];$$

here $T = \mathbf{n}\,\mathrm{rot}\,\mathbf{n}$; $B = (\mathrm{rot}\,\mathbf{n}) \times \mathbf{n}$ and K_{11}, K_{22}, K_{33} are the splay, twist and bend nematic-like elastic constants, respectively. For the x and y components of $\boldsymbol{\Gamma}^{el.}$ ($\Gamma_x^{el.}, \Gamma_y^{el.}$) we find

$$\left.\begin{aligned} \Gamma_x^{el.} &= (K_{22}\cos^2\omega + K_{33}\sin^2\omega)\sin\omega\,\partial^2\theta/\partial y^2 = -K_\omega^+ \sin\omega p^2\theta, \\ \Gamma_y^{el.} &= -(K_{22}\cos^2\omega + K_{33}\sin^2\omega)\cos\omega\partial^2\theta/\partial y^2 = K_\omega^+ \cos\omega p^2\theta, \end{aligned}\right\} \tag{16}$$

where

$$K_\omega^+ = K_{22}\cos^2\omega + K_{33}\sin^2\omega \quad \text{and} \quad \theta = \theta_0 \cos(py)$$

and p is the wavevector of the sinusoidal propagation of the distortion (as a result of $\mathbf{n}$ and flow coupling) in the y direction.

The dielectric torque can be written as

$$\boldsymbol{\Gamma}^{diel.} = \mathbf{P} \times \mathbf{E}, \tag{17}$$

since

$$\mathbf{P} = \varepsilon_0 \boldsymbol{\chi} \mathbf{E} \quad \text{and} \quad \boldsymbol{\chi} = \boldsymbol{\varepsilon} - 1.$$

$\Gamma_x^{\text{diel.}}$ is

$$\Gamma_x^{\text{diel.}} = P_y E_z - P_z E_y = \varepsilon_0(\varepsilon_2 - \varepsilon_3)\sin\omega\cos\omega E E_x + \varepsilon_0(\varepsilon_3\sin^2\omega + \varepsilon_2\cos^2\omega - \varepsilon_1)E E_y - \varepsilon_0(\varepsilon_3 - \varepsilon_1)\theta\cos\omega E^2 \tag{18}$$

and

$$\Gamma_y^{\text{diel.}} = P_z E_x - P_x E_z = \varepsilon_0(\varepsilon_1 - \varepsilon_3\cos^2\omega - \varepsilon_2\sin^2\omega)E E_x - \varepsilon_0(\varepsilon_2 - \varepsilon_3)\sin\omega\cos\omega E E_y - \varepsilon_0(\varepsilon_3 - \varepsilon_1)\theta\cos\omega E^2. \tag{19}$$

The viscous torque, using [29], is

$$\boldsymbol{\Gamma}^{\text{visc.}} = \mathbf{n} \times (\gamma_1 \boldsymbol{\Omega} + \gamma_2 \mathbf{A}\mathbf{n}), \tag{20}$$

where γ_1, γ_2 are the Leslie coefficients, and

$$\boldsymbol{\Omega} = \dot{n} - \tfrac{1}{2}(\text{rot}\,\mathbf{V} \times \mathbf{n})$$

with $\mathbf{V}$ the fluid velocity. Since $\dot{n} = (0, 0, \dot{\theta})$ and

$$\tfrac{1}{2}(\text{rot}\,\mathbf{V} \times \mathbf{n}) = \tfrac{1}{2}(0, 0, V_{z,y}\sin\omega;$$

$$\boldsymbol{\Omega} = (0, 0, \dot{\theta} - \tfrac{1}{2}\sin\omega V_{z,y});\ A = (0, 0, \tfrac{1}{2}\sin\omega V_z).$$

So

$$\Gamma_x^{\text{visc.}} = \gamma_1\dot{\theta}\sin\omega - (\gamma_1 - \gamma_2)/2(\sin^2\omega\,\partial V_z/\partial y), \tag{21}$$

$$\Gamma_y^{\text{visc.}} = -\gamma_1\dot{\theta}\cos\omega + (\gamma_1 - \gamma_2)/4(\sin 2\omega\,\partial V_z/\partial y). \tag{22}$$

Now

$$\left.\begin{aligned} -\Gamma_x^{\text{visc.}} &= \Gamma_x^{\text{el.}} + \Gamma_x^{\text{diel.}} \\ -\Gamma_y^{\text{visc.}} &= \Gamma_y^{\text{el.}} + \Gamma_y^{\text{diel.}}, \end{aligned}\right\} \tag{23}$$

From equations (21) and (22)

$$-\Gamma_x^{\text{visc.}} = -\gamma_1\sin\omega[\dot{\theta} - (\gamma_1 - \gamma_2)/2\gamma_1(\sin\omega V_{z,y})].$$

$$-\Gamma_y^{\text{visc.}} = \gamma_1\cos\omega[\dot{\theta} - (\gamma_1 - \gamma_2)/2\gamma_1(\sin\omega V_{z,y})].$$

Using equations (16), (18) (19) and substituting in equation (23), we obtain

$$\frac{\Gamma_x^{\text{diel.}}}{\sin\omega} + \frac{\Gamma_y^{\text{diel.}}}{\cos\omega} = 0. \tag{24}$$

From this equation

$$E_x = \frac{\cos\omega}{\sin\omega}\,\frac{2(\varepsilon_3 - \varepsilon_1)\theta\sin\omega E + [2(\varepsilon_2 - \varepsilon_3)\sin^2\omega + (\varepsilon_1 - \varepsilon_2)]E_y}{2(\varepsilon_2 - \varepsilon_3)\cos^2\omega + (\varepsilon_1 - \varepsilon_2)}$$

and

$$E_{x,y} = \frac{\cos\omega}{\sin\omega}\,\frac{2(\varepsilon_3 - \varepsilon_1)\sin\omega E\psi + [2(\varepsilon_2 - \varepsilon_3)\sin^2\omega + (\varepsilon_1 - \varepsilon_2)]E_{y,y}}{2(\varepsilon_2 - \varepsilon_3)\cos^2\omega + (\varepsilon_1 - \varepsilon_2)}; \tag{25}$$

and so

$$\frac{\Gamma_y^{\text{diel.}}}{\cos\omega} = \varepsilon_0\varepsilon_\omega E^2\theta - \varepsilon_0(\varepsilon_\omega/\sin\omega)E E_y.$$

Equation (13) can be written in our geometry (see figure 1) as

$$\rho dV_z/dt = -\mathrm{Div}\,(\rho VV)_z + (\mathrm{Div}\,\sigma)_z + (\mathrm{Div}\,\sigma')_z + qE, \tag{26}$$

where

$$\mathrm{Div}\,(\rho \mathbf{VV})_z = \partial/\partial y\,(\rho V_y V_z) = 0,$$

$$(\mathrm{Div}\,\boldsymbol{\sigma})_z = \partial/\partial y\,(\sigma_{y,z}) = \partial/\partial y \sum_l (\partial h_{el}/\partial n_{l,y}) n_{l,z} = 0.$$

Consequently,

$$\rho \partial V_z/\partial t = \partial/\partial y\,(\sigma'_{y,z}) + qE. \tag{27}$$

After some hydrodynamic considerations along the lines of the Ericksen–Leslie nematodynamics, we obtain, for $\sigma_{y,z}$,

$$\begin{aligned}\sigma'_{y,z} = {} & (\gamma_2 - \gamma_1)/2(\dot{\theta} \sin \omega) + (\gamma_2 - \gamma_1)/4\,(\sin^2 \omega V_{z,y}) \\ & + (\beta_2 - \gamma_2)/4(\sin^2 \omega V_{z,y}) + (\alpha_4/2) V_{z,y},\end{aligned} \tag{28}$$

where α_4, β_2 are also the nematic-like viscosity coefficients. Using equation (21), $\sigma'_{y,z}$ becomes

$$\sigma'_{y,z} = (\gamma_2 - \gamma_1)/2\gamma_1(\Gamma_x^{\mathrm{visc.}}) + \eta' \sin^2 \omega V_{z,y}, \tag{29}$$

where

$$\eta' = [\gamma_1(\beta_2 + 2\alpha_4/\sin^2 \omega) - \gamma_2^2]/4\gamma_1 \tag{30}$$

and could be adopted as an effective viscosity.

Since

$$\partial/\partial y(\sigma'_{y,z}) + qE = 0$$

$$(\gamma_2 - \gamma_1)/2\gamma_1 \Gamma_{x,y}^{\mathrm{visc.}} + \eta' \sin^2 \omega V_{z,y,y} + qE = 0. \tag{31}$$

Using again equation (21) and its y derivatives, we found

$$\sin^2 \omega V_{z,y,y} = 2\gamma_1/(\gamma_1 - \gamma_2)(\sin \omega \dot{\psi}) - 2/(\gamma_1 - \gamma_2)(\Gamma_{x,y}^{\mathrm{visc.}}). \tag{32}$$

Substituting this into equation (31), we obtain

$$\frac{\gamma_2 - \gamma_1}{2\gamma_1} \Gamma_{x,y}^{\mathrm{visc.}} + \frac{\eta' 2\gamma_1}{\gamma_1 - \gamma_2} \sin \omega \dot{\psi} - \frac{2\eta'}{\gamma_1 - \gamma_2} \Gamma_{x,y}^{\mathrm{visc.}} + qE = 0. \tag{33}$$

After some algebra

$$\Gamma_{x,y}^{\mathrm{visc.}} = \frac{2\gamma_1(\gamma_1 - \gamma_2)}{(\gamma_1 - \gamma_2)^2 + 4\eta'\gamma_1} \left(\frac{2\gamma_1 \eta'}{\gamma_1 - \gamma_2} \sin \omega \dot{\psi} + qE \right). \tag{34}$$

Differentiating the torque balance equation

$$\Gamma_x^{\mathrm{visc.}} = (K^+ p^2 + \varepsilon_0 \varepsilon_\omega E^2)\theta \sin \omega - \varepsilon_0 \varepsilon_\omega E E_y,$$

we obtain

$$\Gamma_{x,y}^{\mathrm{visc.}} = (K^+ p^2 + \varepsilon_0 \varepsilon_\omega E^2) \sin \omega, \psi - \varepsilon_0 \varepsilon_\omega E E_{y,y}. \tag{35}$$

Further, substituting equation (34) into equation (35) and using $E_{y,y}$ from equation (7), we find

$$\dot{\psi}-\frac{1}{\eta_0}[K_\omega^+ p^2+\varepsilon_0\varepsilon_\omega(1-\varepsilon_\omega)E^2]\psi+\frac{1}{\eta_0}\frac{(\nu+\varepsilon_\omega/\tilde{\varepsilon}_\omega)}{\sin\omega}qE=0, \tag{36}$$

where

and

$$\left.\begin{aligned}\eta_0&=2\gamma_1^2\eta'/(\gamma_1-\gamma_2)^2+4\eta'\gamma_1\\ \nu&=2\gamma_1(\gamma_1-\gamma_2)/(\gamma_1-\gamma_2)^2+4\eta'\gamma_1.\end{aligned}\right\} \tag{37}$$

Consequently, equation (36) is an equation of the director curvature at the electrohydrodynamic instability in S_C. We compare this equation with that for the director curvature in the corresponding nematic instability, i.e. with the equation

$$\dot{\psi}+\frac{1}{T}\psi+qE/\eta=0,$$

where the time-dependent quantity

$$T^{-1}=\lambda(E^2+E_0^2)$$

appears as a relaxation time for the director curvature, and

$$\lambda=-\frac{\Delta\varepsilon}{4\pi}\frac{\varepsilon_\perp}{\varepsilon_\parallel}\left(\frac{1}{\gamma_1}+\frac{1}{\eta_0}\right).$$

So, for the smectic C instability the relaxation time for the director curvature is

$$T_C^{-1}=-\eta_0^{-1}[K_\omega^+ p^2+\varepsilon_0\varepsilon_\omega(1-\varepsilon_\omega)E^2] \tag{38}$$

and

$$\eta^{-1}=\eta_0^{-1}(\nu+\varepsilon_\omega/\tilde{\varepsilon}_\omega)/\sin\omega \tag{39}$$

can be accepted as an effective viscosity coefficient often considered in the simplified situation as the rotational viscosity ν.

Consequently, equations (8) and (36) are two coupled equations for the charge density q and the director curvature ψ in the regime of the 'initial' domains, which are linear in q and ψ. The experiment considered by us is an AC electric field $E(t)=E_m\exp(i\bar{\omega}t)$ and we can rewrite equations (8) and (36). Following the procedure described in [28] for the nematic instability in the conducting regime, we obtain the threshold electric field for the 'initial' domain appearing as

$$E_{th}^2(t)=E_0^2(1+\bar{\omega}^2\tau_C^2)/[(\lambda^*)^2-(1+\bar{\omega}^2\tau_C^2)], \tag{40}$$

where E_0 is the DC electric field value and $\bar{\omega}$ is the electric field frequency. It is seen from this equation that the threshold field depends only on two parameters which are characteristic for the S_C materials: τ_C and the dimensionless coefficient $(\lambda^*)^2$, which is a combination of the dielectric constants, electroconductivity and viscosity reflecting the biaxiality of the smectic C.

$$(\lambda^*)^2=\sigma_C\tau_C/\lambda_C\eta, \tag{41}$$

where

$$\sigma_C\tau_C=\tilde{\varepsilon}_\omega\varepsilon_0/\sigma_2[(\Delta\sigma_b+\sigma_2\varepsilon_\omega\sin^2\omega)/\sin\omega]$$

and

$$\lambda_C \eta = -[K_\omega^+ p^2 + \varepsilon_\omega \varepsilon_0 (1-\varepsilon_\omega)] \sin\omega / [(v+\varepsilon_\omega)/\tilde{\varepsilon}_\omega].$$

Consequently, for the parameter $(\lambda^*)^2$ which is analogous to the ξ^2 parameter, known as the Orsay parameter for nematics, we obtain

$$(\lambda^*)^2 = -\varepsilon_0 \tilde{\varepsilon}_\omega [\Delta\sigma_b (\tilde{\varepsilon}_\omega v + \varepsilon_\omega) + \sigma_2 \varepsilon_\omega \tilde{\varepsilon}_\omega^2 \sin^2\omega (1+\varepsilon_\omega)] / \sigma_2 \sin^2\omega \varepsilon_\omega [K_\omega^+ p^2 + \varepsilon_\omega \varepsilon_0 (1-\varepsilon_\omega)]. \quad (42)$$

2.2. *The high frequency fundamental domain regime*

The experimental details for this regime are given in [6, 7] and here we only consider the theoretical aspects. As was demonstrated in [6, 7], the deformation participating in the electrohydrodynamic instability regime is the bend, which is visualized by the domain line texture, and resembles the dielectric regime in a nematic, For a description of the instability we choose another laboratory cartesian frame where the ox axis points in the rubbing direction and z is parallel to the layer plane (see figure 2). θ and φ are the polar and azimuthal angles expressing the **n** deviation from the easy direction x. According to the local biaxiality characteristic for the S_C, the dielectric tensor in a local frame of reference has three different eigenvalues ε_1, ε_2 and ε_3 with the principal axes: $\varepsilon_3 \to \mathbf{n}$; $\varepsilon_2 \to \mathbf{n} \times (\mathbf{N} \times \mathbf{C})$, and $\varepsilon_1 \to \mathbf{N} \times \mathbf{C}$. The difference with the initial domain regime is that the **n** fluctuations now restricted and propagate mainly in the xz plane, and θ (x) is the fluctuation angle.

ε can be written in the xyz system as

$$\varepsilon \approx \begin{pmatrix} \varepsilon_3 & (\varepsilon_2 - \varepsilon_3)\varphi & (\varepsilon_3 - \varepsilon_1)\theta \\ (\varepsilon_2 - \varepsilon_3)\varphi & \varepsilon_2 & 0 \\ (\varepsilon_3 - \varepsilon_1)\theta & 0 & \varepsilon_1 \end{pmatrix}. \quad (43)$$

The principal axes of σ from the phase symmetry should be: $\sigma_3 \to \mathbf{N}$; $\sigma_2 \to \mathbf{C}$ and $\sigma_1 \to \mathbf{N} \times \mathbf{C}$, and as in the initial regime, we keep in mind that the electroconductivity is much less perpendicular to the smectic layers than inside the layers. Thus we can

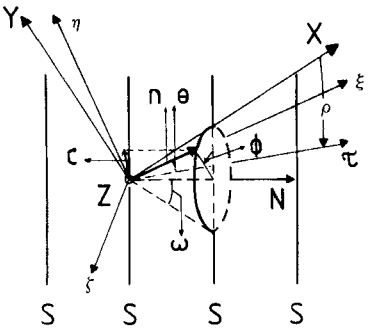

Figure 2. The smectic C director **n** presentation at the fundamental domain regime. The xyz coordinate system is rotated in order ox to coincide with **R** the rubbing direction. The other parameters of the system are the same as those of figure 1.

assume that $\sigma_3 \approx 0$, and again using $\sin\phi = \sin\theta/\sin\omega$ for small θ we obtain for $\boldsymbol{\sigma}$ in the xyz system

$$\boldsymbol{\sigma} \approx \begin{pmatrix} \sigma_2 \sin^2\omega & \frac{1}{2}\sigma_2 \sin 2\omega & -(\sigma_1 - \sigma_2)\theta \\ \frac{1}{2}\sigma_2 \sin 2\omega & \sigma_2 \cos^2\omega & -(\sigma_1 - \sigma_2)\operatorname{cotan}\omega\theta \\ -(\sigma_1 - \sigma_2)\theta & -(\sigma_1 - \sigma_2)\theta \operatorname{cotan}\theta & \sigma_1 \end{pmatrix}, \tag{44}$$

where we assume $\sigma_1 - \sigma_2 = \Delta\sigma_b$ as a first approximation for the anisotropy of the electroconductivity. Applying the continuity equation for the electric current **J** and for the electric induction D, we have equations (3) and (4). Taking ε and σ from equations (43) and (44), we obtain

$$\left.\begin{aligned} J_x &= \sigma_2 \sin^2\omega E_x + \sigma_2(\sin 2\omega/2)E_y - \Delta\sigma_b \theta E_z, \\ D_x &= \varepsilon_3 E_x + (\varepsilon_2 - \varepsilon_3)\varphi E_y + (\varepsilon_3 - \varepsilon_1)\theta E_z. \end{aligned}\right\} \tag{45}$$

Substituting $\Delta\varepsilon$ and $\psi = \partial\theta/\partial x$, the local director curvature, we obtain

$$\dot{q} + (q/\varepsilon_3\varepsilon_0)(\sigma_2 \sin^2\omega) - [\Delta\varepsilon/\varepsilon_3(\sigma_2 \sin^2\omega) + \Delta\sigma_b]E\psi = 0. \tag{46}$$

The charge relaxation time in the S_C phase is now

$$\tau_c^+ = \sigma_2 \sin^2\omega/\varepsilon_0\varepsilon_3 \tag{47}$$

and

$$\sigma_c^+ = -[\Delta\varepsilon/\varepsilon_3(\sigma_2 \sin^2\omega) + \Delta\sigma_b]. \tag{48}$$

Following the description in § 2.1 for the curvature director equation, we have used the equation of motion (26). Since the smectic C flow is restricted inside the layer $\mathbf{K} \cdot \mathbf{N} = 0$, where **K** is the wavevector of the curvature director fluctuation. The fluid motion velocity is

$$V_z(x, y) = V_z \cos(K_x x + K_y y).$$

Taking the polar components of $\mathrm{N} \rightarrow N(\cos\omega, \sin\omega, 0)$, see figure 3, and

$$K_x \cos\omega + K_y \sin\omega = 0,$$

we find $K_x/K_y = -\tan\omega$. Equation (26) can be written as

$$\rho\, \partial V_z/\partial t = \partial/\partial x \sigma'_{x,z} + \partial/\partial_y \sigma'_{y,z} + qE_z. \tag{49}$$

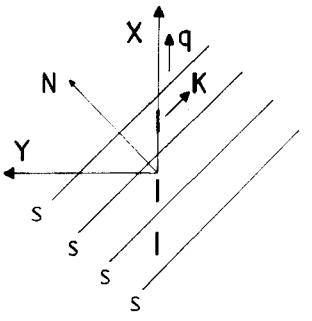

Figure 3. The fluid motion presentation. The smectic C flow is restricted inside the layers. **K** is the wavevector of the curvature director fluctuation.

For small θ and φ the director components are

$$\mathbf{n}(\cos\theta\cos\varphi, \cos\theta\sin\varphi, \sin\theta) \approx (1, \varphi, \theta).$$

After some hydrodynamic consideration as in § 2.1, we obtain, for $\sigma'_{x,z}$,

$$\sigma'_{x,z} = \frac{\gamma_2 - \gamma_1}{2}\dot{\theta} + \frac{(\gamma_1 - \gamma_2)^2}{4\gamma_1} V_{z,x} + \frac{(2\alpha_4 + \beta_2)\gamma_1 - \gamma_2^2}{4\gamma_1} V_{z,x}, \tag{50}$$

where $\gamma_1, \gamma_2, \alpha_4, \beta_2$ are the nematic-like viscosity coefficients, and η' is the combination

$$\eta' = (2\alpha_4 + \beta_2)\gamma_1 - \gamma_2^2/4\gamma_1, \tag{51}$$

which is accepted as an effective viscosity. In order to achieve the torque balance in the instability regime, we write, having in mind that the only non-zero component of V is $V_z(x, t)$, the components of $\Gamma^{\text{visc.}}$

$$\Gamma^{\text{visc.}} = \{0, -[\gamma_1\dot{\theta} - (\gamma_1 - \gamma_2)/2V_{z,x}], \gamma\dot{\varphi}\}.$$

We are interested in $\Gamma_y^{\text{visc.}}$ which is coupled to the flow

$$\Gamma_y^{\text{visc.}} = [\gamma_1\dot{\theta} - (\gamma_1 - \gamma_2)/2V_{z,x}]. \tag{52}$$

Now $\sigma'_{x,z}$ can be expressed by $\Gamma_y^{\text{visc.}}$

$$\left.\begin{aligned} &\sigma'_{x,z} = (\gamma_1 - \gamma_2)/2\gamma_1(\Gamma_y^{\text{visc.}}) + \eta' V_{z,x}, \\ &\partial/\partial_x\sigma'_{x,z} + \partial/\partial y\sigma'_{y,z} + qE_z = \rho\dot{V}_z = 0, \\ &(\gamma_1 - \gamma_2)/2\gamma_1(\Gamma_{y,x}^{\text{visc.}}) + \eta' V_{z,xx} + (\alpha_4/2)V_{z,yy} + qE_z = 0, \end{aligned}\right\} \tag{53}$$

The elastic torque $\Gamma^{\text{el.}} = \mathbf{n} \cdot \mathbf{h}_{\text{el.}}$ with the y component

$$\Gamma_y^{\text{el.}} = -K_B\theta_{,xx} = K_B q_x^2\theta, \tag{54}$$

where K_B is the Saupe director curvature elastic constant for S_C, which in our case is a nematic-like bend constant participating in the fundamental electrohydrodynamic instability regime [7] and $q_x = \pi x/d$.

The dielectric torque and its y component can be written as

$$\Gamma_y^{\text{diel.}} = -\varepsilon_0\Delta\varepsilon E^2(\theta + E_x/E). \tag{55}$$

The x derivatives of the torques can now be expressed as functions of the charge q and the curvature ψ

$$-\Gamma_{y,x}^{\text{visc.}} = \Gamma_{y,x}^{\text{el.}} + \Gamma_{y,x}^{\text{diel.}}. \tag{56}$$

The torque balance equation can be written as

$$\gamma_1\dot{\psi} - (\gamma_1 - \gamma_2)/2(V_z q_x^2) = (K_B q_x^2 - \varepsilon_0\Delta\varepsilon E^2)\psi - \varepsilon_0\Delta\varepsilon E E_{xx}. \tag{57}$$

From equation (53) substituting $(\alpha_4/2)V_{z,yy} \to q_x^2 V_z/\tan^2\omega$ and since $q_y = -q_x/\tan\omega$, we obtain

$$(\gamma_1 - \gamma_2)/2\gamma_1(\Gamma_{y,x}^{\text{visc.}}) + (\eta' + \alpha_4/2\tan^2\omega)V_z q_x^2 + qE = 0. \tag{58}$$

Now $\eta'' = \eta' + \alpha_4/2\tan^2\omega$ and substituting in this equation

$$V_z q_x^2 = \frac{\gamma_1 - \gamma_2}{2\gamma_1\eta''}[(K_B q_x^2 - \varepsilon_0\Delta\varepsilon E^2)\psi - \varepsilon_0\Delta\varepsilon E E_{xx}] - qE/\eta''. \tag{59}$$

Inserting in the torque balance equation from equation (58), we have

$$\gamma_1\dot{\psi}-\frac{(\gamma_1-\gamma_2)}{4\gamma,\eta''}[(K_Bq_x^2-\varepsilon_0\Delta\varepsilon E^2)\psi-\varepsilon_0\Delta\varepsilon EE_{xx}]-\frac{\gamma_1-\gamma_2}{2\eta''}qE$$
$$=(K_Bq_x^2-\varepsilon_0\Delta\varepsilon E^2)\psi-\varepsilon_0\Delta\varepsilon EE_{x,x}$$

and expressing

$$E_{x,x}=\varepsilon_3^{-1}(q/\varepsilon_0-\Delta\varepsilon\psi E),$$

we obtain

$$\gamma_1\dot{\psi}-A(K_Bq_x^2+\varepsilon_0\Delta\varepsilon(\Delta\varepsilon/\varepsilon_3-1)E^2]\psi+(A\Delta\varepsilon/\varepsilon_3-(\gamma_1-\gamma_2)/2\eta'')qE=0, \tag{60}$$

where

$$A=1+(\gamma_1-\gamma_2)^2/4\gamma_1\eta''; \quad \eta''=\eta'+(\alpha_4/2)\operatorname{cotan}^2\omega.$$

This equation expresses the director curvature at the fundamental instability regime. Comparing this equation with its equivalent for the nematic instability, we find for the director curvature the relaxation time

$$T^{-1}=-A[K_Bq_x^2+\varepsilon_0\Delta\varepsilon(\Delta\varepsilon/\varepsilon_3-1)E^2] \tag{61}$$

and

$$\eta^{-1}=A(\Delta\varepsilon/\varepsilon_3)-(\gamma_1-\gamma_2)/2\eta''. \tag{62}$$

As it was shown in [6, 7], the initial and fundamental domain regimes are analogous to the conducting and dielectric regimes in nematics with $\Delta\varepsilon<0$. The difference is, however, in the instability in S_C phases with negative dielectric anisotropy, as there is no cut-off frequency as in nematics. There is a frequency range $(\nu''-\nu')$ where the instability regime can be considered as a mixture of initial and fundamental domain regimes and the domain structures is two dimensional. The width of this transition range depends on the temperature and the cell thickness and, for example, for a 50 μm thick cell of HOBA at 96·5°C is 12 Hz. The initial domain regime slowly disappears above this range and at frequency ν''' also depending on the temperature and the thickness only manifested the fundamental regime. So, the description of the transition range between the two instabilities is very complicated and our description in §§ 2.1 and 2.2 are for the ranges far from the mixed range. So, for frequencies $\nu>\nu'''$ we can find [28] for the threshold field expression

$$E_{th}^2(t)=\mathscr{L}_m[(\lambda^+)^2]\bar{\omega}/\lambda^f, \tag{63}$$

where

$$\mathscr{L}_m=\lambda^fE_m^2/2\bar{\omega} \quad \text{and} \quad (\lambda^+)^2=\tau_C^+\sigma_C^+/\lambda^f\eta,$$
$$\tau_C^+\sigma_C^+=-\varepsilon_0\Delta\varepsilon+\varepsilon_0\varepsilon_3\Delta\sigma_b/\sigma_2\sin^2\omega,$$
$$\lambda^f\eta=-\varepsilon_0\Delta\varepsilon/\varepsilon_3(1/\gamma_1+1/\eta_0'')(A\Delta\varepsilon/\varepsilon_3-\gamma_1-\gamma_2/2\varepsilon_3\eta''),$$

for small

$$\Delta\varepsilon\to(\Delta\varepsilon/\varepsilon_3\ll1); \quad \eta=\eta'=2\alpha_4+\beta-\gamma_1/4$$

and

$$\lambda^f\eta=-\varepsilon_0\Delta\varepsilon/4\varepsilon_3(2\alpha_4+\beta-\gamma_1).$$

So, for the parameter $(\lambda^+)^2$ which is an analogue of ξ^2 the Orsay parameter, we obtain

$$(\lambda^+)^2=\left(-\varepsilon_0\Delta\varepsilon+\frac{\varepsilon_0\varepsilon_3\Delta\sigma_b}{\sigma_2\sin^2\omega}\right)\Big/\left[-\frac{\varepsilon_0\Delta\varepsilon(2\alpha_4+\beta-\gamma_1)}{4\varepsilon_3}\right].$$

2.3. *The influence of the magnitude and the sign of the dielectric anisotropy on the electrooptic behaviour of S_C*

Let us adopt the theory just presented and especially the threshold field equation to the case where the dielectric constant anisotropy varies with a broad range of different signs and magnitudes. The first step is to adopt the threshold field equation (40) for the initial regime (which is often dominant) for both signs of the anisotropy $\Delta\varepsilon$. So, equation (40) can be written in the form where the role of the dielectric anisotropy is more apparent [28]

$$E_{th}^2=G_0(1+\bar{\omega}^2\tau_C^{2)}/\Delta\varepsilon\bar{\omega}^2\tau_C^2+\chi, \tag{64}$$

where

$$G_0^2=\pi^2\varepsilon_3K_B/d^2\sin^2\omega\varepsilon_1, \tag{65}$$

where K_B is an effective elastic constant, namely the Saupe S_C constant for the director curvature at pure dielectric reorientation, d is the cell thickness and

$$\chi=-\Delta\varepsilon[(\lambda^*)^2-1] \tag{66}$$

is an analogue of the Helfrich parameter in nematics [30]. We have the possibility to connect the thresholds for the instability when $\bar{\omega}$ is sufficiently small or $\bar{\omega}\to0$, i.e. $E_{th_0}^2$ and that of the Fredericksz transition E_f which presents the hydrodynamic and dielectric reorientation, respectively. The threshold for the Fredericksz transition E_f is obtained as $E_f^2=G_0^2/\Delta\varepsilon$ from equation (64) after replacing χ from equation (66) and putting $(\lambda^*)^2=0$ implying that there is no hydrodynamic torque acting on the director. From the same equation (64) we can obtain at $(\bar{\omega})^2=0$ the domain instability threshold at frequencies tending to zero, i.e. $E_{th_0}^2=G_0/\chi$. Now substituting equation (65) into equation (64) as well for $(\lambda^*)^2=0$, we obtain

$$E_f=\pi/d\sin\omega(K_B\varepsilon_3/\varepsilon_1\Delta\varepsilon)^{1/2}. \tag{67}$$

This equation is valid only for the case where the smectic layer normal (for planar orientation) lies in the substrate plane (i.e. the book-shelf geometry). We have a direct ratio between E_f and E_{th_0} from equations (65) and (66) since $E_{th_0}^2=G_0^2/\chi$. Consequently $E_{th_0}^2=E_f^2/[1-(\lambda^*)^2]$ from which

$$1-(\lambda^*)^2=E_f^2/E_{th_0}^2. \tag{68}$$

By measuring E_f^2 and $E_{th_0}^2$, we can determine K_B and $(\lambda^*)^2$. The ratio of E_f and E_{th_0} values depends on the absolute value of $(\lambda^*)^2$. So, from equation (68) it follows that the values of $(\lambda^*)^2$, for which the instability is possible, are: $(\lambda^*)<0$; $(\lambda^*)^2=0$; $0<(\lambda^*)^2<1$

(i) $(\lambda^*)^2=0$

$$E_f=E_{th_0}$$

the electrohydrodynamic instability torque disappears and the Fredericksz transition predominates over the instability.

(ii) $(\lambda^*)^2 < 0$

$$E_f = aE_{th_0}; \quad a > 0, \quad E_f > E_{th_0}$$

here the larger the absolute value of $(\lambda^*)^2$, the higher the threshold E_f over E_{th_0}.

(iii) $0 < (\lambda^*)^2 < 1$

$$E_f = E_{th_0}/b, \quad b > 0, \quad E_f < E_{th_0}$$

here the instability threshold is higher than the Fredericksz one. Presumably in this situation the electric field puts the director in a position from which the hydrodynamic torques initiate the instability.

3. Experimental results and discussion

Using the notation [28] known for nematics and concerning the character of the instabilities on the sign and the magnitude of the dielectric anisotropy, we can summarize the corresponding dependences for the smectic C system. We choose only the geometry $\mathbf{n}_0 \perp \mathbf{E}$, where $\mathbf{n}_0$ is the initial director. In our experiment it corresponds to a planar orientation with an electric field applied perpendicular to the substrate plane. We shall consider the $\Delta\varepsilon$ values in the range of large negative to large positive. The first marginal value of $\Delta\varepsilon$ (starting from zero) where the instability cannot develop, we denote by $\Delta\varepsilon^0$. This value corresponds to $(\lambda^*)^2 = 1$, as follows from equation (68) since $E_{th}^2 \to \infty$, below $\Delta\varepsilon^0$ the system is absolutely stable. In order to determine the $\Delta\varepsilon^0$ value, we have used equation (42). From this equation taking $0 < \omega \approx \pi/4$, we find

$$\Delta\varepsilon^0 = -(\mu\Delta\sigma_b)/1 - \mu\sigma_1 < 0,$$

where μ is a dimensionless ratio involving the friction coefficients γ_1, η' and $\gamma_1 - \gamma_2 > 0$. The other values or limits of $\Delta\varepsilon$ where the character of the instability changes we denote by 0, $\Delta\varepsilon'$ and $\Delta\varepsilon''$. Obviously, in these points $(\lambda^*)^2 = 0$ and only a conducting regime ($\Delta\varepsilon = 0$) or pure Fredericksz regime ($\Delta\varepsilon'$ and $\Delta\varepsilon''$) develop. So, the condition $(\lambda^*)^2 = 0$ from equation (41) leads to the values of $\Delta\varepsilon'$ and $\Delta\varepsilon''$. Using equation (41), it is seen that the two roots in the solutions correspond to the zeros of equation (12) and of η^{-1} (see equation (39)). The first value $\Delta\varepsilon > 0$, i.e. $\Delta\varepsilon'$ is

$$\Delta\varepsilon' = \Delta\sigma_b(1 - 2\cos^2\omega)/\sin^2\omega\sigma_2 > 0.$$

The second higher value is

$$\Delta\varepsilon'' = [\nu(1 - 2\cos^2\omega)2(\cos^2\omega + 1)]/2\varepsilon_1\cos^2\omega + \varepsilon_3 > 0.$$

For $(\lambda^*)^2 = 0$ the torque due to the Carr–Helfrich effect vanishes and from equation (64) the threshold independence of the frequency ($E_f^2 = G_0^2/\Delta\varepsilon$) is obtained. So returning to equation (64), we find the following types of electrooptic behaviour upon increasing $\Delta\varepsilon$.

(i) $\Delta\varepsilon < \Delta\varepsilon^0$, complete stability

(ii) $\Delta\varepsilon^0 < \Delta\varepsilon < 0$, instability expressed by domain lines (similar to the initial domain lines [5–7]), conducting regime and dynamic scattering at higher fields. Dielectric regime is possible at higher frequency (like the fundamental one [5–7]). Such a dielectric regime in this case occurs above the critical frequency region ($\nu'' - \nu'$) where the two regimes occur simultaneously. The dielectric regime is possible only in this range

(iii) $0 < \Delta\varepsilon < \Delta\varepsilon'$

According to the same threshold condition in equation (64), the threshold field is an increasing function of the frequency. Two subregions are possible:

(*a*) $0<\Delta\varepsilon<\frac{1}{3}\Delta\varepsilon'$

when the field is increased at constant $\bar{\omega}$, a low frequency (conducting) domain regime is observed first and this is followed by dynamic scattering:

(*b*) $\frac{1}{3}\Delta\varepsilon'<\Delta\varepsilon<\Delta\varepsilon'$

Only a conducting regime expressed by domains is possible since before achieving turbulence, a reorientation of the director takes place. The threshold field is an increasing function of $\bar{\omega}$. The dielectric regime does not appear.

(iv) $\Delta\varepsilon'<\Delta\varepsilon<\Delta\varepsilon''$

The threshold field is a decreasing function of the frequency.

(v) $\Delta\varepsilon>\Delta\varepsilon''$

The threshold field is also an increasing function of the frequency. At these values of $\Delta\varepsilon$ only a reorientation of the director **n** takes place with an increasing voltage and no instability appears since the dielectric torque is a stabilizing one. It is clear that with these conditions the conducting regime may indeed extend to arbitrary high frequency until a certain frequency $\bar{\omega}$ where the dispersion of the dielectric constant would become important.

In order to verify these theoretical conclusions, the role of the magnitude and sign of $\Delta\varepsilon$ as shown here as well as the tilt angle role, we have chosen a series of substances displaying S_{C_2} and S_{C_1} phases. The substances and some of their characteristic parameters taken mainly from the work of Pelzl *et al.* [2] and by [6] are listed in the table. Five substances have been chosen in order to check the condition for $\Delta\varepsilon$ and ω values.

We describe briefly the electrooptical behaviour of the substances shown in the table in an AC electric field and compare their behaviour with conditions (i) to (v), as well as the fundamental threshold conditions expressed in the theoretical part. We have used a 20 μm thick liquid crystal cell for all substances; the planar orientation was achieved by SiO treated substrates. The textual analysis was accomplished with a polarizing microscope equipped with a Linkam hot stage.

3.1. *The substance* C_6

C_6 was investigated in detail by [2] in the frequency range 1–2 kHz. Here we shall use a wider frequency range in order to obtain the dependence $E_{th}^2=f(\bar{\omega}^2)$ which gives us a possibility to compare the experimental results in the line of the electrooptic character presented by the notations (i)–(v). In figure 4 we present this dependence at fixed temperature in the S_C phase. For low frequencies (below 5 kHz) we observed (increasing the electric field value for $\bar{\omega}=$ const.) first a Fredericksz transition described in [2] and at higher field value $E_{th_1}>E_f$ an instability picture (see figure 5). This instability is an initial type instability with domain linewidth comparable with the cell thickness. At $E_{th_2}>E_{th_1}$ a dynamic scattering mode appears, as seen from figure 4 in the frequency range $0<\bar{\omega}<5$ kHz.

E_{th}^2 is a decreasing function of $\bar{\omega}^2$ with a conducting regime character. The value $E_{th_0}=G_0/\chi$ is shown in figure 4. The Fredericksz threshold value does not depend on

The compounds and some of their characteristic parameters.

Compounds and transition temperatures	T/°C	$\Delta\varepsilon$	ω°	τ_{rise}/ms	τ_{decay}/ms	ν/mPa s^{-1}
C_1 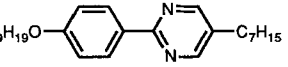	47	0·47	20			
C 45·5°C S_C 51°C S_A 56°C N 69·5°C I	50	0·46	12·5			
C_2 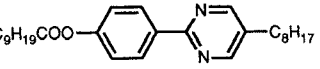	50	0·12	13·5			
C 42°C S_C 55·5°C N 59·8°C I						
C_6 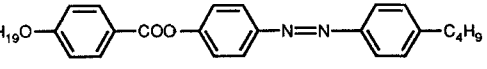						
C 84·5°C S_C 95·3°C N 193·5°C I	93	0·27	15	6	5	1·6
HOAB 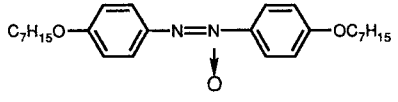						
C 74·6°C S_C 95·0°C N 124·3°C I	88	−0·02	38·5			
HOBA 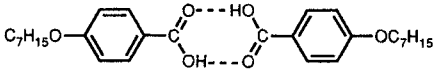	96·5	−0·028	45	20	8	
C 92°C S_C 98°C N 146°C I				for in. regime $E=0{\cdot}410^{V/cm}$		

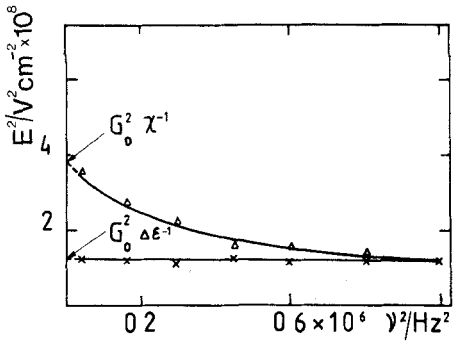

Figure 4. The dependence $E_{th}^2 = f[(\bar{\omega})^2]$ at 92°C for C_6: ×, $(E_f)^2$; Δ, $(E_{th}^{in})^2$; $G_0^2/\chi \rightarrow (E_{th_0}^{in})^2$; $G_0^2/\Delta\varepsilon \rightarrow E_f^2$; $E_{th}^{in} > E_f$; $(E_{th}^{in})^2$ decreasing function of $(\bar{\omega})^2$. The symbol "in" means initial domains.

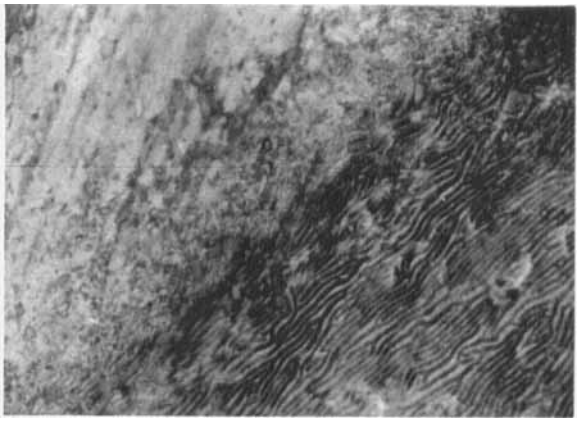

Figure 5. The initial type domains in C_6, at 92°C, $d = 20\,\mu m$; $(E_{th}^{in})^2 = 1{\cdot}56 \times 10^8 V^2/cm^2$, $\nu^2 = 3{\cdot}6 \times 10^3\,Hz^2$.

the frequency and is marked as $G_0^2/\Delta\varepsilon$. So, we have observed case (iv). In order to compare the threshold E_f and E_{th_0} on the basis of equation (68), we obtain $E_f < E_{th_0}$ resulting in $0 < (\lambda^*)^2 < 1$. Probably in case 3.1 the electric field puts the **n** director in a position from which the hydrodynamic flow develops creating an instability which is an initial domain regime in this experiment.

3.2. *The substance* C_2

The dependence $E_{th}^2 = f(\bar{\omega}^2)$ for C_2 is shown in figure 6, here we also have $E_f < E_{th_0}$. In this case the Fredericksz transition is discontinuous and before going to the instability regime we observe a few changes of colour with distinct optical states. The instability in C_2 (see figure 7) appears at higher voltages than those for C_6. The instability here is expressed by domain lines similar to that of the initial domain regime but growing from one centre (see figure 7). So, the domain lines follow the direction of the confocal growth which is from one centre. Up to 2 kHz E_{th} is an increasing function of $\bar{\omega}$ and corresponds to the conducting regime. According to the classification

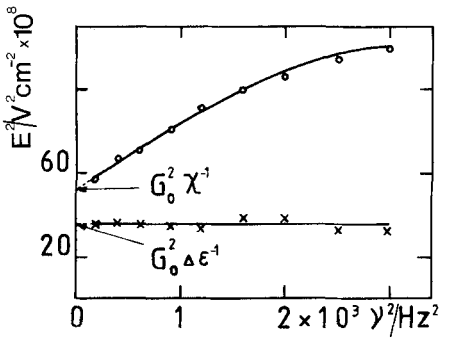

Figure 6. The dependence $E_{th}^2 = f[(\bar{\omega})^2]$ for C_2 at 50°C; ×, $(E_f)^2$; ○, $(E_{th}^{in})^2$; $(E_{th}^{in})^2$ increasing function of $(\bar{\omega})^2$.

Figure 7. The initial domains in C_2, at 65°C, with $d = 20\,\mu m$, $\nu^2 = 0{\cdot}9 \times 10^3\,Hz^2$, $(E_{th}^{in})^2 = 121 \times 10^8\,V^2/cm^2$.

presented here the electrooptics of C_2 below 2 kHz correspond to the case where $0 < \Delta\varepsilon < \Delta\varepsilon'$, i.e. to (iii).

3.3. *The substance HOAB*

This substance forms local single monocrystals similar to those of HOBA [7]. The dependence $E_{th}^2 = f(\bar{\omega}^2)$ is presented in figure 8, from where it is seen that $E_f < E_{th_0}$. Two regimes of electrohydrodynamic instability have been found. The initial at $\nu = \bar{\omega}/2\pi$ between 0 and ν'. The domain lines in this regime are shown in figure 9, they are parallel to the elongated local monocrystal and their width is comparable to the cell thickness d. At frequency $\nu > \nu'$ a two dimensional domain structure starts where fundamental stripes [6] appear and superimpose on the initial ones. The angle between the initial and the fundamental stripes is 60°. The simultaneous existence of the initial and fundamental domains presents a texture (a two dimensional diffraction grating) similar to that of HOBA [5, 6, 31]. At $\nu > \nu'''$ the initial domains disappear and only fundamental stripes are seen. The value of the frequency range $\Delta\nu = \nu'' - \nu'$ depends on the temperature of the smectic C phase and the cell thickness. The width of the

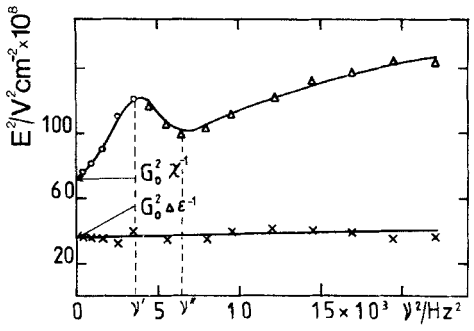

Figure 8. The dependence $E_{th}^2 = f[(\bar{\omega})^2]$ for HOAB at 92°C. $E_f < E_{tho}^{in}$. The initial domains below ν' and fundamental above ν'' ×, E_f^2; ○, $(E_{th}^{in})^2$; Δ, $(E_{th}^{fun})^2$, where fun means fundamental domains.

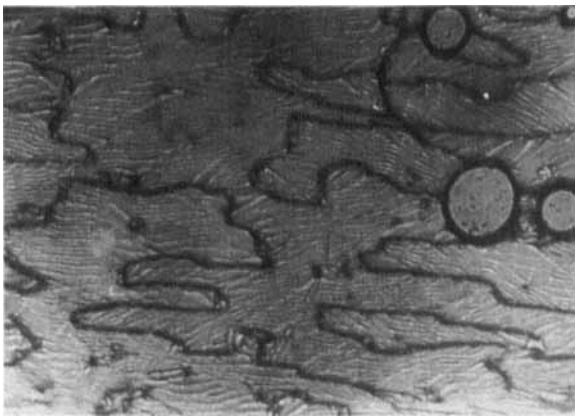

Figure 9. The initial domains for HOAB at 117°C, with $d = 20\,\mu m$, $\nu^2 = 0{\cdot}9 \times 10^3\,Hz^2$, $(E_{th}^{in})^2 = 81 \times 10^8\,V^2/cm^2$.

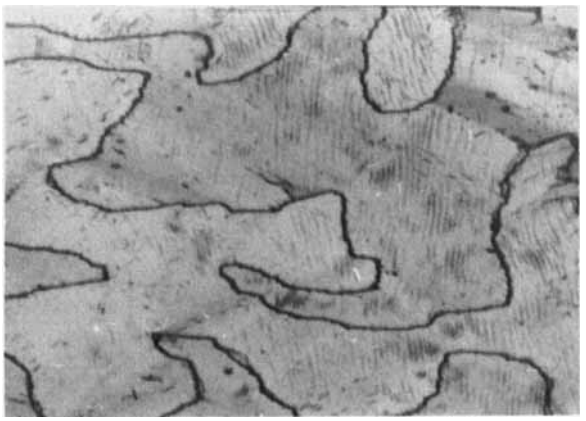

Figure 10. The fundamental domains for HOAB, at 117°C, with $d = 20\,\mu m$, $\nu^2 = 6{\cdot}4 \times 10^3\,Hz^2$, $(E_{th}^{fun})^2 = 100 \times 10^8\,V^2/cm^2$.

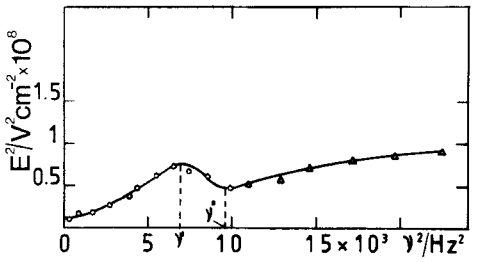

Figure 11. The dependence $E_{th}^2=f[(\bar{\omega})^2]$ for HOBA. ○, $(E_{th}^{in})^2$; Δ $(E_{th}^{fun})^2$.

fundamental domains (see figure 10) is less than the cell thickness. The instability of HOAB can be related to the case $0<\Delta\varepsilon<\frac{1}{3}\Delta\varepsilon'$, i.e. (iii(*a*)), but it is peculiar since a coexistence of all electric instabilities, Fredericksz transition, initial and fundamental domains, is observed.

3.4. *The HOBA substance*

The dependence $E_{th}^2=f(\bar{\omega}^2)$ for HOBA is given in figure 11. As seen, HOBA indicates only instability regimes and not Fredericksz transitions. The electrohydrodynamic instability of HOBA is extensively described in [5–7], but here we can conclude that this substance may be related to the condition (ii), i.e. $\Delta\varepsilon^0<\Delta\varepsilon<0$, where conducting and dielectric regimes are developed. The local single monocrystals in HOBA form more easily than in HOAB presumably due to the larger tilt angle, ω.

3.5. *The substance* C_1

According to the scheme proposed for the character of the electrooptic response depending on $\Delta\varepsilon$, substance C_1 can be related to the case $\Delta\varepsilon>\Delta\varepsilon''$.

In conclusion, we have developed a theoretical description for the electrohydrodynamic instability in a smectic C which allows us to connect this phenomenon with the pure dielectric reorientation (the Fredericksz transition). The conditions were found under which the dielectric reorientation can precede the instability upon increasing the field or the instability can develop directly. The role of the anisotropy $\Delta\varepsilon$ is very important in this respect but it is not unique. The tilt angle ω determines the character of the instability developed to a great extent. The dielectric reorientation can be considered as a priority of substances with smaller tilt angles while the instability develops more easily in substances with a larger and a temperature independent tilt angle ω. For example, HOAB and HOBA possess almost equal $\Delta\varepsilon$ but dielectric reorientation develops only in HOAB where ω is smaller. As shown in the theoretical part, the dielectric relaxation time, which expresses the distribution of the electric charge in the layers, is smaller at larger tilt angles. Consequently, the coupling of the charge flow with the director curvature ψ is faster at such angles ensuring rapid instability development without dielectric reorientation.

Finally, the present paper is a first attempt to account for the biaxiality typical for smectic C materials and to obtain the fundamental equations for charge flow and director curvature coupling. Measurements of the three principal values $\varepsilon_1, \varepsilon_2, \varepsilon_3$ as well as σ_1, σ_2, σ_3 are necessary in order to verify more precisely the basic equations presented here.

The work is supported by the Science Foundation under contract No. 480.

References

[1] PELZL, G., KOLBE, P., PREUKSCHAS, U., DIELE, S., and DEMUS, D., 1979, *Molec. Crystals liq. Crystals*, **53**, 167.
[2] PELZL, G., SCHILLER, P., and DEMUS, D., 1987, *Liq. Crystals*, **2**, 131.
[3] VISTIN, L. K., and KAPUSTIN, A. P., 1968, *Sov. J. Crystallogr.*, **13**, 349.
[4] GOSCIANSKI, M., 1975, *Philips Res. Rep.*, **30**, 37.
[5] SIMOVA, P., PETROV, M., and KIROV, N., 1977, *Molec. Crystals liq. Crystals*, **42**, 295.
[6] PETROFF, B., PETROV, M., SIMOVA, P., and ANGELOV, A., 1978, *Ann. Phys.*, **3**, 331.
[7] PETROV, M., and DURAND, G., 1981, *J. Phys. Lett., Paris*, **42**, L-519.
[8] SAUPE, A., 1969, *Molec. Crystals liq. Crystals*, **7**, 59.
[9] ORSAY LIQUID CRYSTAL GROUP, 1971, *Solid St. Commun.*, **9**, 653.
[10] MARTIN, P., PARODI, O., and PERSHAN, P., 1972, *Phys. Rev.* A, **6**, 240.
[11] DE VRIES, A., 1979, *Liquid Crystals—The Fourth State of Matter*, edited by F. D. Saeva (Marcel Dekker Inc.), p. 1.
[12] PETROV, M., LEVELUT, A. M., and DURAND, G., 1982, *Molec. Crystals liq. Crystals Lett.*, **82**, 221.
[13] CLARK, N. A., and LAGERWALL, S. T., 1986, *Proc. 6th International Display Research Conference*, Tokyo, Japan, p. 456.
[14] RIEKER, T. P., CLARK, N. A., SMITH, G. S., PARMER, D. S., SIROTA, E. B., and SAFINYA, C. R., 1987, *Phys. Rev. Lett.*, **59**, 2658.
[15] OUCHI, Y., TAKANO, H., TAKEZOE, H., and FUKUDA, A., 1987, *Jap. J. appl. Phys.*, **26**, L21.
[16] OUCHI, Y., LEE, J., TAKEZOE, H., FUKUDA, A., KONDO, K., KITAMURA, T., and MUKOH, A., 1988, *Jap. J. appl. Phys.*, **27**, L725.
[17] CLARK, N. A., and RIEKER, T. P., 1988, *Phys. Rev.* A, *Rap. Commun.*, **37**, 1053.
[18] SHINGU, T., TSUCHIYA, T., OUCHI, Y., TAKEZOE, H., and FUKUDA, A., 1986, *Jap. J. appl. Phys.*, **25**, L206.
[19] NAKAGAWA, M., 1989, *Molec. Crystals liq. Crystals*, **174**, 65.
[20] OUCHI, Y., TAKANO, H., TAKEZOE, H., and FUKUDA, A., 1988, *Jap. J. appl. Phys.*, **27**, 1.
[21] OUCHI, Y., LEE, J., TAKEZOE, H., FUKUDA, A., KONDO, K., KITAMURA, T., and MUKOH, A., 1988, *Jap. J. appl. Phys.*, **27**, L1993.
[22] TAYLOR, T. R., FERGASON, J. L., and ARORA, S. L., 1970, *Phys. Rev. Lett.*, **24**, 359.
[23] BUKA, A., and BATA, L., 1979, *Molec. Crystals liq. Crystals.*, **49**, 159.
[24] KRESSE, H., WIGELEBEN, A., and DEMUS, D., 1980, *Kristall Tech.*, **15**, 341.
[25] CARR, E. F., 1970, *Phys. Rev. Lett.*, **24**, 807.
[26] RAPINI, A., 1972, *J. Phys., Paris*, **33**, 237.
[27] MEIROVICH, E., LUZ, Z., and ALEXANDER, S., 1977, *Phys. Rev.* A, **15**, 408.
[28] DUBOIS-VIOLETTE, E., DE GENNES, P. G., and PARODI, O., 1971, *J. Phys., Paris*, **32**, 305.
[29] ERICKSEN, L. J., 1960, *Archs. ration. Mech. Analysis*, **4**, 231; PARODI, O., 1970, *J. Phys., Paris*, **31**, 581.
[30] HELFRICH, W., 1969, *J. chem. Phys.*, **51**, 4092.
[31] PETROV, M., and SIMOVA, P., 1984, *Cryst. Res. Tech.*, **19**, 691.